# Urban Density, Green Space, and Land Surface Temperature: A Metro Vancouver Case Study using Satellite Imagery

Isaac Qi, Aidan O'Brien, Yunke Li, Janine Jia

FRE 527 - Environmental Economics and Policy: Empirical Analysis

February 24th, 2026

## Motivation

High-density metropolitan areas are systematically associated with elevated land surface temperatures (LST), a key feature of the urban heat island effect (Yang et al., 2016). This phenomena is attributed to vegetation being replaced by concrete and other heat-retaining surfaces. Elevated LST has consequences for both human and ecological health, including increased heat stress, higher energy demand, and reduced quality of life (Singh et al., 2020).

Urban green spaces are proposed as a natural cooling solution. Vegetation reduces surface temperatures through shading and evapotranspiration, and studies show that greener areas are generally cooler (Aram et al., 2019). Wu et al., 2021 found that even in high-density cities, very small "pocket" green spaces can measurably cool surrounding areas, although their cooling effects are typically weaker and more localized than those of large parks. This suggests that greenspace can provide thermal benefits even under dense urban conditions; however, the magnitude and spatial extent of cooling may vary substantially depending on the surrounding context. In very dense areas, vegetation is often fragmented and tightly surrounded by roads, buildings, and

other heat-retaining surfaces, which may limit how much cooling it can realistically provide. While previous studies show that greenspace size and configuration matter (Aram et al., 2019; Wu et al., 2021), it is still unknown whether the overall urban density of an area changes how effective urban greenspaces are in reducing LST.

Understanding whether the relationship between greenspace and temperature varies across different levels of urban density is essential for informing urban climate adaptation strategies. If cooling effects differ systematically by density, urban planning policies should account for these heterogeneous effects rather than assuming a constant benefit of urban greenspaces.

Building on the aforementioned motivations, this project seeks to understand: *How does the relationship between urban greenspace and land surface temperature vary across high-density vs lower-density metropolitan areas, particularly Metro Vancouver?* Rather than assuming that greenspace has a uniform impact across the city, the focus is on whether vegetation reduces temperatures differently in more densely built environments compared to less dense areas. To explore this, the analysis examines pixel-level temperature variation within Greater Vancouver and tests whether the magnitude of greenspace cooling depends on local urban intensity. In addition, the study considers alternative ways of measuring both temperature (e.g., extreme heat metrics) and urban density to assess the robustness of the interaction. Lastly, the study examines how different greenspace land cover types vary in their effectiveness in reducing land surface temperature. By centering the analysis on this interaction between density and vegetation, the goal is to better understand how urban structure shapes the effectiveness of greenspace as a heat mitigation strategy.

## Methodology

*Dataset Characteristics*

This study combines five geospatial datasets in Google Earth Engine (GEE) to characterize how land cover and urban form relate to summer surface heat in Greater Vancouver. Initial criteria for choosing the datasets were to (1) provide a heat outcome variable (satellite land surface temperature), (2) represent land cover at sufficiently fine resolution to capture fragmented urban greenspace, and (3) provide control covariates that explain spatial temperature gradients. The spatial extent is the FAO GAUL (2015) second-level administrative boundary for “Greater Vancouver,” clipped to the polygon in all processing steps. The temporal focus is July 1–31 in 2023–2025, capturing peak summer conditions when urban heat patterns are most pronounced.

All datasets were accessed through GEE for accessibility and familiarity. Land surface temperature (LST), the main dependent variable, is measured using the VIIRS VNP21A1D.002 Daytime Land Surface Temperature product (Hulley & Hook, 2023), derived from thermal infrared observations collected by the VIIRS sensor onboard the Suomi NPP satellite; it provides daily global LST at ~1 km spatial resolution from 2012 onward. We chose this dataset as land surface temperature was precisely the variable of interest, and that alternative temperature measures, such as cooling degree days, can be derived from raw LST values. Urban greenspace is identified using ESA WorldCover v200 (Zanaga et al., 2021), a 10 m global land cover product with a 2021 reference year derived from Sentinel satellite imagery; its fine spatial resolution is well suited to Greater Vancouver because it captures both large parks and smaller fragmented vegetated areas within dense neighborhoods. In addition, previous

familiarity of this dataset contributed to the selection decision. In this study, greenspace is defined as tree cover, shrubland, grassland, and cropland, where we summarized greenspace as the fraction of each 1 km grid cell covered by the aggregate greenspace. The individual landcover fractions were also retained.

Urban density is measured using the Gridded Population of the World dataset (GPWv4.11), produced by CIESIN and constructed by spatially allocating census counts to raster grid cells (CIESIN, 2018). The GPW population density layer is provided at 30 arc-second resolution (approximately 1 km at the equator) for five-year snapshots from 2000 to 2020; although this does not exactly match 2023-2025, population density changes gradually over time and is used here as a reasonable proxy for structural urban intensity in Greater Vancouver. This variable was ultimately chosen over built-up land cover from the ESA WorldCover dataset given its policy relevance of heat stress in populated areas affecting more people, though built-up was retained in the analysis process. Elevation is included to control for topographic temperature gradients particularly to address the mountainous terrain affecting LST readings; we chose the GMTED2010 (Danielson & Gesch, 2011) dataset which has ~231 spatial resolution and was last updated in 2010. A summary of the dataset descriptions and data quality are included in Table 1 below.

| Data Product | Spatial Resolution | Temporal Coverage | Derived From | Data Accuracy |
|---|---|---|---|---|
| NASA VIIRS VNP21A1D.002<br><br>(Hulley & Hook, 2023) | 1 km | 2012 - Present (Daily) | thermal infrared observations collected by the VIIRS sensor aboard the Suomi NPP satellite | RMSE of 1.5 K, bias less than 0.5 K |
| ESA WorldCover v200 | 10 m | 2021 (Annual) | Sentinel 1 and Sentinel 2 satellite composite | 76.7% global overall accuracy |

| | | | | |
|---|---|---|---|---|
| (Zanaga et al., 2021) | | | | |
| GPWv4.11<br><br>(CIESIN, 2018) | ~927 m | 2010 - 2020 (5-year) | CIESIN census spatial interpolation | Not applicable |
| GMTED2010<br><br>(Danielson & Gesch, 2011) | ~231 m | 2010 | Shuttle Radar Topography Mission (SRTM) data, Spot 5 Reference3D data, and data from the Ice, Cloud, and land Elevation Satellite (ICESat) | Global accuracy of 6 m RMSE |

*Data Processing*

The study area was defined using the FAO GAUL (2015) second-level administrative boundary for “Greater Vancouver,” and all spatial layers were clipped to this polygon. Land surface temperature (LST) was extracted from the NASA VIIRS VNP21A1D daytime product for July 1-31 in 2023-2025 at the product’s ~1 km grid. Daily LST images were filtered using a mask retaining positive Kelvin values, converted from Kelvin to degrees Celsius, and summarized into three per-pixel metrics for July of each year: (1) mean July LST (average across all July days), (2) July p90 LST (the 90th percentile temperature across July in each pixel), and (3) Cooling Degree Days (CDD) using 18°C as a baseline, computed as the sum of July LST_day − 18°C; values outside −10°C to 70°C were filtered to limit outliers in the CDD calculation.

Land cover predictors were derived from ESA WorldCover v200 (2021) at 10 m by converting relevant land cover classes to binary masks: tree cover, shrubland, grassland, cropland, and built-up; a greenspace mask was defined as any of tree, shrub, grass, or crop. Each 10 m binary layer was spatially aggregated to the 1 km analysis grid using a mean reducer, yielding fractional variables representing the share of each 1 km cell occupied by each land cover class, and reprojected to match the

VIIRS grid. To assess the effect of the overall size of greenspaces, neighbourhood mean fractions for tree, grass, and total greenspace were also computed on the 1 km grid using a 1500 m circular kernel. The neighbourhood mean fraction value does not include the center pixel. Population density (GPWv4.11, 2020) was resampled using bilinear interpolation for alignment and clipped to the study region, and elevation was derived from the GMTED2010 data product and aggregated to 1 km using its mean.

Finally, all variables were stacked and sampled at 1 km resolution across the study area. Latitude and longitude coordinates were retained for each pixel, and the resulting dataset was exported as a CSV for statistical analysis.

## Data Description

*Descriptive Statistics*

After preprocessing and exporting the 1 km pixel sample from GEE, the final analysis dataset contains 4,680 observations across the Greater Vancouver study region. Table 1 summarizes the main variables used in the analysis, including July mean LST, July p90 LST, and July cooling degree days (CDD) for 2023-2025, along with land-cover fractions, elevation, and population density. Greenspace fraction is high on average, likely reflecting the large forested and mountainous areas in the north, while built-up fraction is comparatively low on average but spatially concentrated. The temperature variables show year-to-year differences in July heat conditions.

Table 2: Descriptive Statistics - Metro Vancouver (2023-2025)

| Variable | Mean | SD | Min | Max | N |
|---|---|---|---|---|---|
| CDD 2023 (°C-days) | 236.104 | 138.418 | 6.57 | 583.98 | 4680 |
| CDD 2024 (°C-days) | 160.831 | 74.784 | 9.35 | 386.28 | 4680 |
| CDD 2025 (°C-days) | 189.352 | 110.73 | 6.29 | 474.53 | 4680 |
| LST Mean 2023 (°C) | 29.001 | 5.924 | 18.022 | 42.692 | 4680 |
| LST Mean 2024 (°C) | 30.163 | 5.265 | 18.03 | 43.937 | 4680 |
| LST Mean 2025 (°C) | 28.573 | 5.872 | 11.553 | 42.975 | 4680 |
| LST 90th percentile 2023 (°C) | 33.663 | 6.255 | 21.45 | 49.51 | 4680 |
| LST 90th percentile 2024 (°C) | 34.503 | 5.9 | 20.83 | 51.33 | 4680 |
| LST 90th percentile 2025 (°C) | 33.125 | 6.089 | 22.03 | 49.27 | 4680 |
| Built-up Fraction | 0.133 | 0.217 | 0 | 0.948 | 4680 |
| Crop Cover Fraction | 0.019 | 0.08 | 0 | 0.808 | 4680 |
| Elevation (m) | 322.828 | 401.734 | -0.111 | 1668.831 | 4680 |
| Grass Cover Fraction | 0.164 | 0.219 | 0 | 0.983 | 4680 |
| Greenspace Fraction | 0.796 | 0.266 | 0 | 1 | 4680 |
| Population Density | 905.562 | 1958.722 | 0 | 27365.553 | 4680 |
| Shrub Cover Fraction | 0 | 0 | 0 | 0.008 | 4680 |
| Tree Cover Fraction | 0.613 | 0.343 | 0 | 1 | 4680 |

*Data Visualization*

To contextualize the variables spatially, Figure 1 maps ESA WorldCover classes (tree cover, shrubland, grassland, cropland, built-up) at high spatial resolution (10 m) and shows the contrast between the urban sprawl of the metropolitan areas compared to the extensive surrounding vegetation and mountainous northern region.

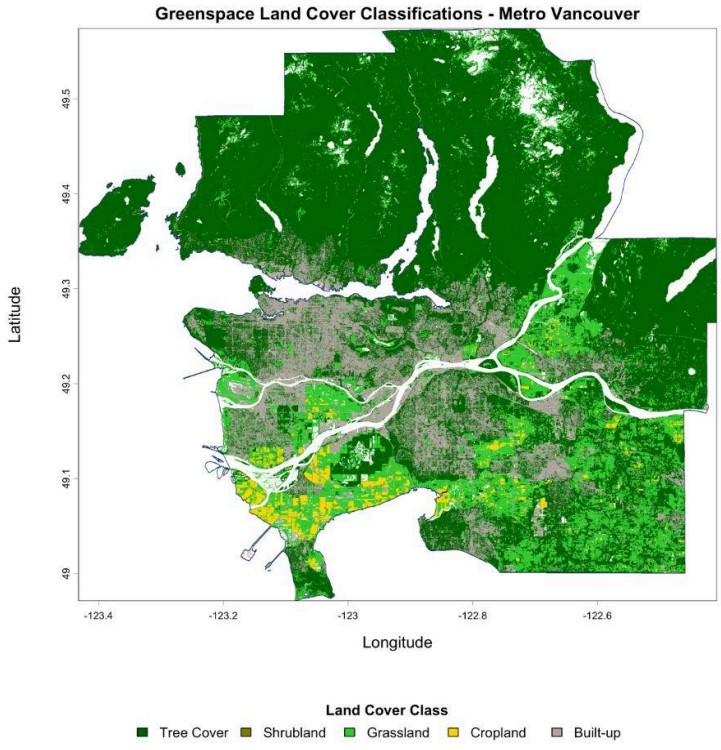


**Fig 1. Greenspace land cover classifications in Metro Vancouver**

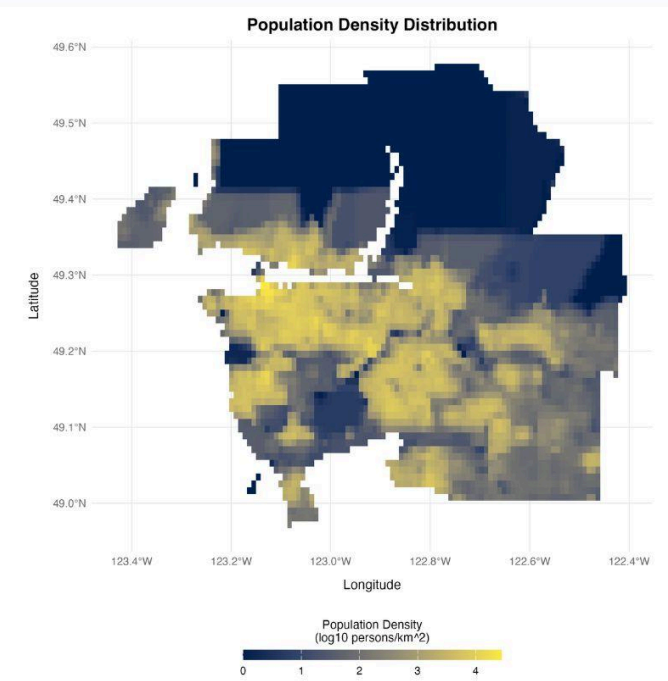


**Fig 2. Population Density Map**

Figure 2 maps population density and visually confirms its close overlap with built-up in fig 1, supporting the use of population density as a proxy for urban intensity while maintaining the policy relevance of human concentration.

Figure 3 presents July 2025 surface-heat patterns using three complementary metrics: mean LST (typical daytime surface heat), 90th percentile LST (extreme heat exposure), and Cooling Degree Days (cumulative heat burden above 18°C). All three maps exhibit highly similar spatial structure, where the same urbanized areas and built-up clusters appear consistently hotter, while less-developed or higher-elevation areas appear cooler.

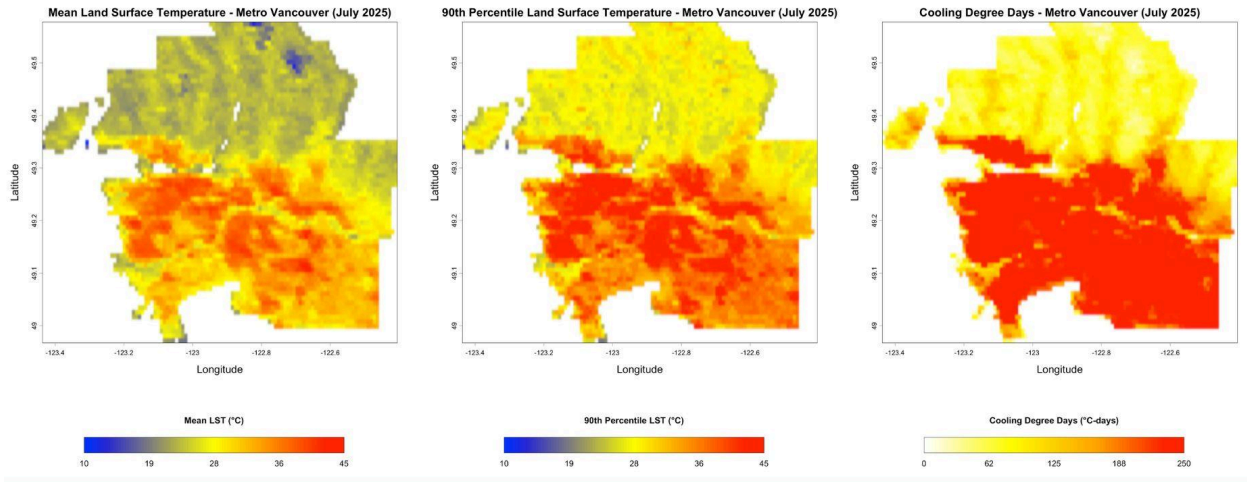


Fig 3. Vancouver temperature variation by mean, 90th percentile, and cooling degree days.

In figure 3, we see that regardless of the temperature metric selected, the northern half of Metro Vancouver is much cooler than the south. Figure 4 maps elevation and visualizes a key confound for interpreting temperature gradients: the cooler northern portion of the study region overlaps strongly with higher elevations, meaning raw temperature differences could reflect topography rather than greenspace or urban form; for this reason, elevation is included as a necessary control in the regression models.

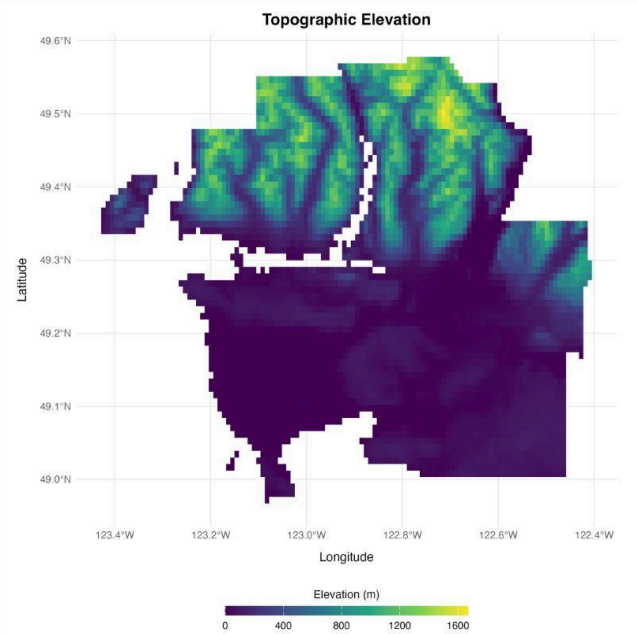


**Fig 4. Vancouver Topographic Elevation Map**

Lastly, we began exploratory work to assess whether neighbouring tree cover differs meaningfully from within-pixel tree cover at the 1 km scale. Figure 5 compares tree cover in the centre pixel to mean tree cover in a 1.5 km surrounding ring, showing broadly similar distributions but also deviations for some locations. The bottom panel summarizes this "neighbourhood effect" (mean − centre), which is centered near zero but has clear tails, suggesting that some pixels are embedded in neighbourhoods that are substantially greener (or less green) than the pixel itself.

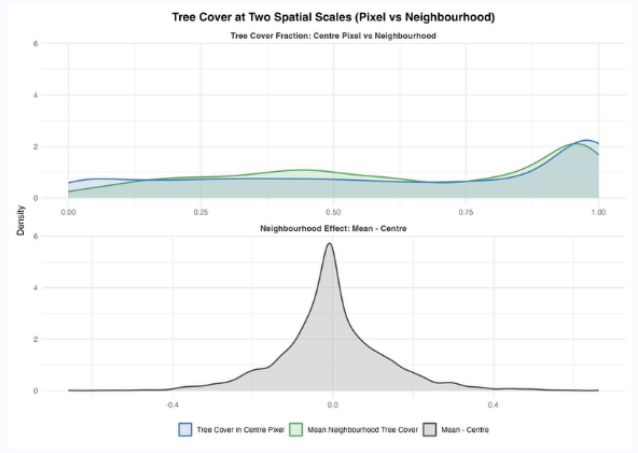


**Fig 5. Neighbouring Tree Effect**

## Results & Interpretation

To test our hypothesis, we performed regression analysis on our data exported from Google Earth Engine. We used three temperature related dependent variables: mean land surface temperature, 90th percentile land surface temperature, and cooling degree days. Our regressors stayed the same for each regression, with particular interest on our main independent variable, the interaction of population density and greenspace percentage. This interaction term allows us to assess the cooling difference between greenspaces across varying population densities.

As seen below, our regressions show similar results regardless of the temperature metric used. As expected, elevation and greenspace percentage have a negative relationship with temperature, but contrary to our expectations, population density does as well. Coefficients on the interaction terms are all positive, which indicates that as population density increases, the cooling effect of greenspace decreases.

OLS Regression: Temperature vs Greenspace

| | Mean LST | 90th percentile LST | CDD |
|---|---|---|---|
| | (1) | (2) | (3) |
| Intercept | 39.771*** | 45.179*** | 384.713*** |
| | (0.489) | (0.486) | (8.932) |
| Elevation | -0.009*** | -0.008*** | -0.193*** |
| | (0.001) | (0.001) | (0.015) |
| Percent Greenspace | -0.090*** | -0.101*** | -1.546*** |
| | (0.006) | (0.006) | (0.102) |
| Population Density (in 1000s) | -0.236*** | -0.298*** | -4.217** |
| | (0.091) | (0.089) | (1.701) |
| Population Density × Greenspace | 0.013*** | 0.015*** | 0.244*** |
| | (0.001) | (0.001) | (0.026) |
| Observations | 1819 | 1819 | 1819 |
| $R^2$ | 0.428 | 0.463 | 0.421 |
| Adjusted $R^2$ | 0.427 | 0.462 | 0.420 |
| Residual Std. Error | 3.233 (df=1814) | 3.327 (df=1814) | 59.651 (df=1814) |
| F Statistic | 308.405*** (df=4; 1814) | 349.173*** (df=4; 1814) | 305.643*** (df=4; 1814) |
| Note: | | | *p<0.1; **p<0.05; ***p<0.01 |

Also of interest is the effect of different types of greenspace on cooling. ESA Worldcover has 4 classifications that we count as greenspace in Greater Vancouver: Tree cover, grassland, shrubland, and cropland. Results can be seen in the table below. In general, we find that of the greenspace land cover types, tree cover is the most effective at reducing temperatures. Cropland is slightly more effective than grassland at reducing temperatures, but they have substantially less cooling power than tree cover. Shrubland, the rarest land cover type in Greater Vancouver, has the smallest cooling power, while still producing a significant negative effect on temperature.

OLS Regression: Temperature vs Greenspace by Type

| | Mean LST | 90th percentile LST | CDD |
|---|---|---|---|
| | (1) | (2) | (3) |
| Intercept | 39.641*** | 45.064*** | 382.470*** |
| | (0.494) | (0.490) | (9.014) |
| Percent Trees | -0.117*** | -0.126*** | -2.056*** |
| | (0.006) | (0.006) | (0.108) |
| Percent Shrubs | -0.000*** | -0.000*** | -0.000*** |
| | (0.000) | (0.000) | (0.000) |
| Percent Grass | -0.055*** | -0.069*** | -0.901*** |
| | (0.007) | (0.007) | (0.122) |
| Percent Crops | -0.076*** | -0.083*** | -1.119*** |
| | (0.010) | (0.011) | (0.179) |
| Elevation | -0.002 | -0.002 | -0.056*** |
| | (0.001) | (0.001) | (0.019) |
| Population Density (in 1000s) | -0.374*** | -0.429*** | -6.869*** |
| | (0.090) | (0.088) | (1.679) |
| Population Density × Greenspace | 0.018*** | 0.021*** | 0.353*** |
| | (0.001) | (0.001) | (0.027) |
| Observations | 1819 | 1819 | 1819 |
| $R^2$ | 0.479 | 0.503 | 0.477 |
| Adjusted $R^2$ | 0.477 | 0.502 | 0.475 |
| Residual Std. Error | 3.087 (df=1812) | 3.201 (df=1812) | 56.759 (df=1812) |
| F Statistic | 226.399*** (df=6; 1812) | 253.933*** (df=6; 1812) | 225.507*** (df=6; 1812) |
| Note: | | | *p<0.1; **p<0.05; ***p<0.01 |

Our results have two policy implications. Firstly, greenspace in Greater Vancouver has different effectiveness at cooling summer temperatures depending on where it is located. Greenspace in less dense areas is capable of producing a greater cooling effect than in areas where population density is high. Secondly, the type of greenspace matters when considering cooling effects. Trees are the most effective, followed by cropland and grass. Shrubland has almost no cooling capacity.

**Limitations & Future Directions**

Several data-related limitations should be acknowledged. First, all variables were aggregated to a 1 km grid to align datasets with different native resolutions. While necessary for consistency, this likely masks fine-scale variation and may underrepresent the cooling effects of small parks or narrow green corridors. Second, there is temporal misalignment across datasets, as land cover and population data precede the temperature data. Third, alternative measures such as built-up land cover fraction may provide a more direct proxy for urban intensity, and future specifications could compare these measures or combine them. Fourth, the current analysis treats each pixel independently, but the exploratory neighbourhood comparisons suggest that land cover in surrounding pixels can differ meaningfully from the centre pixel; a possible extension is to include neighbourhood land-cover measures. Finally, Greater Vancouver's coastal setting introduces additional confounding due to its cooling effect, so future work could incorporate distance-to-coast controls and/or interact coastal proximity with built-up and greenspace measures to better isolate the urban-heat relationship.

**References**


Aram, F., García, E. H., Solgi, E., Mansournia, S. (2019). Urban green space cooling effect in cities. *Heliyon, 5*(4). https://doi.org/10.1016/j.heliyon.2019.e01339

Center for International Earth Science Information Network - CIESIN - Columbia University. (2018). Gridded Population of the World, Version 4 (GPWv4): Population Density, Revision 11. Palisades, NY: *NASA Socioeconomic Data and Applications Center (SEDAC)*. https://doi.org/10.7927/H49C6VHW. Accessed 2026-02-05

Danielson, J.J. & Gesch, D.B. (2011), Global multi-resolution terrain elevation data 2010 (GMTED2010): U.S. Geological Survey Open-File Report 2011-1073, iv, 23 p.; Appendix, https://doi.org/10.3133/ofr20111073.

Hulley, G., & Hook, S. (2023). VIIRS/NPP Land Surface Temperature/Emissivity Daily L3 Global 1km SIN Grid Day V002 [Data set]. *NASA Land Processes Distributed Active Archive Center*. https://doi.org/10.5067/VIIRS/VNP21A1D.002 Date Accessed: 2026-02-05

Singh, N., Singh, S., & Mall, R. K. (2020). Urban ecology and human health: implications of urban heat island, air pollution and climate change nexus. In *Urban ecology* (pp. 317-334). Elsevier.

Wu, C., Li, J., Wang. C., Song, C., Haase, D., Breuste, J., & Finka, M. (2021). Estimating the Cooling Effect of Pocket Green Space in High Density Urban Areas in Shanghai, China. *Frontiers in Environmental Science, 9*. https://doi.org/10.3389/fenvs.2021.657969

Yang, L., Qian, F., Song, D. X., & Zheng, K. J. (2016). Research on urban heat-island effect. *Procedia engineering*, *169*, 11-18.

Zanaga, D., Van De Kerchove, R., Daems, D., De Keersmaecker, W., Brockmann, C., Kirches, G., Wevers, J., Cartus, O., Santoro, M., Fritz, S., Lesiv, M., Herold, M., Tsendbazar, N. E., Xu, P., Ramoino, F., & Arino, O. (2021). ESA WorldCover 10 m 2021 v200 [Dataset]. *Zenodo*. https://doi.org/10.5281/zenodo.7254221

## Appendix

*AI Use Disclaimer*

AI was used in the coding process particularly when we encountered advanced coding needs in GEE (adding thickness to border, fact checking our calculations for CDD and fractions, etc). We also utilized AI in R for some graphical aspects (troubleshooting the white bands previously included in the presentation, recommendations of new packages, stylization of plots). All interpretation and statistical analysis are our own.

*Link to GEE Code:*

*https://code.earthengine.google.com/30844609941b7bd3854081eae05b9ce2*